

Tata Institute of Fundamental Research, Mumbai.

*Passive and Active
cosmic ray shield for low
background
measurements with HPGe
detector.*

*A.Thirunavukarasu
30/11/2009*

Passive and Active cosmic ray shield for low background measurements with HPGe detector

Introduction:

Gamma-ray spectrometry with a high-purity germanium (HPGe) detector is widely used for the identification and activity measurements of radionuclides in a sample, impurity checks of a standard source, determination of emission probabilities in radioactive decay, and low-level counting's. In low-level counting's, a variety of techniques to reduce the background have been employed and makes it possible to radio assay an environmental sample containing a trace of gamma-emitting radionuclides. Here in this project we are making an active cosmic veto and passive lead shielding for HPGe detector to reduce the background radiations.

Preliminary study of components used:

In this experiment we used many electronic components and detector components. In this section some of the components are described in detail regarding their working, performance characteristic etc. A scintillator is material which exhibits the property of luminescence when excited by ionizing radiation. Luminescent materials, when struck by an incoming particle, absorb its energy and scintillate i.e. Re emit the absorbed energy in the form of a small flash of light, typically in the visible range. If it is made of plastic then it is called plastic scintillator (hereafter it is called as simply scintillator).

The advantage of these scintillators is:

- 1) *The decay time of the induced luminescence is very short so that fast pulse can be generated.*
- 2) *The medium is transparent in the optical region and hence ensures good light collection.*
- 3) *The refractive index is close to that of glass and this permits efficient coupling to the photomultiplier tube.*

In order to make the scintillator to be used for proper scientific studies, we need to couple a photo multiplier (PMT) tube on the sides of scintillator. This PMT absorbs the light emitted by the scintillator and converts into pulse signal with the help of High voltage (HV) given as input (The HV applied is in the range of 0 to -2Kv). This HV is applied to the HV input of the PMT and its necessary because it accelerates the electrons produced by photoelectric effect on the PMT. Fig-1 clearly indicates the process in a scintillation detector.

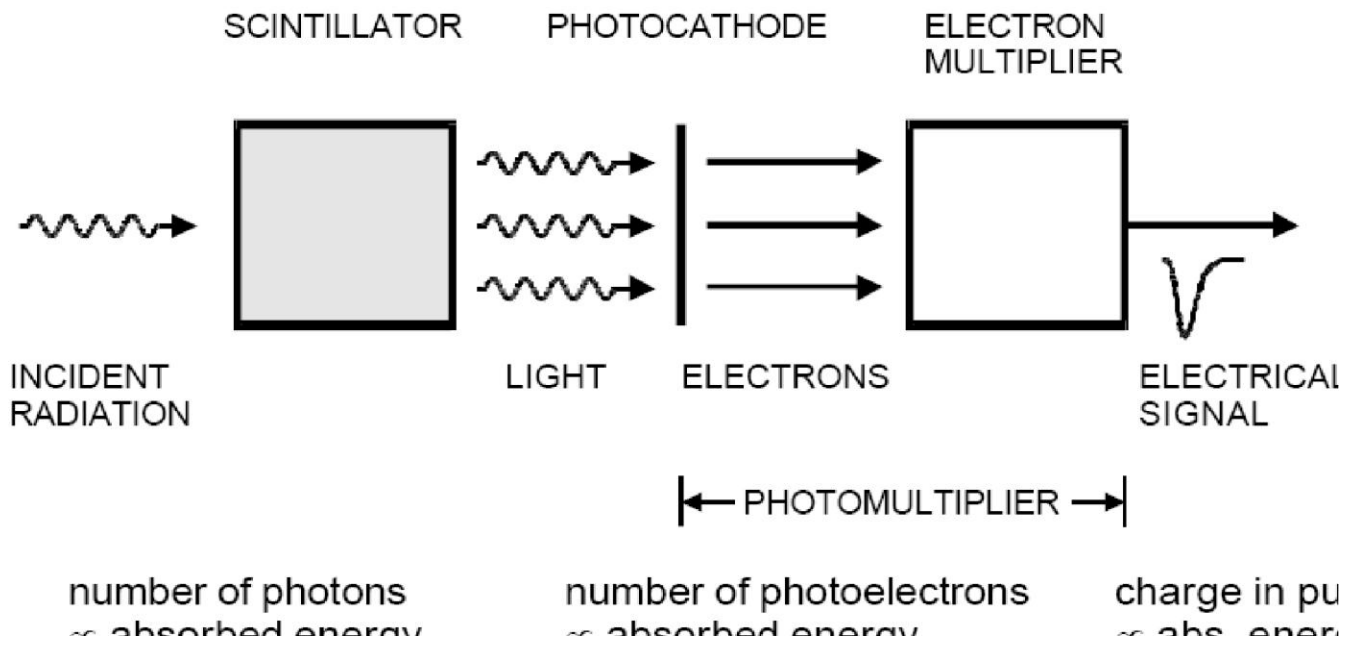


Fig-1: Process in a scintillator and Photo multiplier tube.

In this project as a first step, we analyzed the timing pulse characteristic of the scintillator as a function of HV with the help of cobalt 60 source placed on the bar. Before that we studied the PMT parts and coupled the scintillator(square bar) with one PMT on both sides after doing the initial preparations(i.e. cleaning the surfaces of scintillator and PMT,wrapping white(inside) and black(outside) sheet on the sides of the scintillator).

The PMT has 2 HV inputs (Both connected internally for cascading mode), 2 Anode and Diode output. For setting up the circuit the HV is applied to the HV input terminal and the Anode is connected to the input of the oscilloscope.

Then both the PMT are biased individually and analyzed.

For PMT-A: (PMT-A & PMT-B are just for identification)

Serial no :	High voltage (KV)	Anode Pulse height (mv)	Rise time (ns)	Fall time(ns)
1	1.5	44	2.5	10
2	1.6	70	2.5	10
3	1.7	180	2.5	10
4	1.8	200	2.5	10
5	1.9	400	2.5	10
6	2.0	680	2.5	10

Table 1a: Pulse height variation as a function of applied voltage for PMT-A.

For PMT-B:

Serial no :	High voltage (KV)	Anode pulse height (mv)	Rise time (ns)	Fall time(ns)
1	1.5	60	2.5	7.5
2	1.6	32	3	10
3	1.7	32	3	10
4	1.8	56	3	10
5	1.9	80	2	6
6	2.0	100	2	8

Table 1b: Pulse height variation as a function of applied voltage for PMT-B.

Here the Rise and fall time of both the PMT's were not same because of the different internal gain of the individual PMT.

As a next step, we made some analysis on the Position Vs Time response of the scintillator with the same source. Here, we varied the position of the source kept on the bar. Now the two PMT's are cascaded (by connecting the remaining input of first PMT to the one of the 2 inputs of second PMT) and the anode output of the two PMT's were taken separately and analyzed (without pulse shaping)(see table-2) in the two different channels of the oscilloscope keeping the bias as constant (see fig-2).

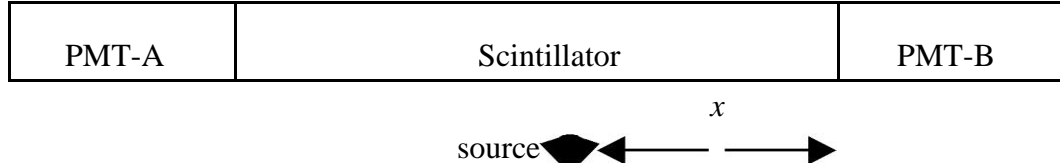


Fig-2: A schematic of variation of position of the source.

Cascaded: HV= -1.8Kv Initial distance of source from PMT-B (X) =44cm

Serial no:	Distance of source from PMT-B	Anode Pulse height (PMT-A)	Anode Pulse height (PMT-B)
1	0	280	40
2	X/4	320	32
3	X/2	360	28
4	3X/4	440	24
5	X	480	24

Table 2: Variation of Pulse height for both PMT as a function of Distance.

After this we did some pulse shaping exercises to get familiarize with pulse shaping procedure. In this exercise the anode output of the PMT- A is send to Timing filter amplifier (TFA) and from there to CFD and to the start of the TAC. Similarly for the PMT-B the anode output was send to the TFA and from there to constant fraction discriminator (CFD) and to the stop of the Time to analog converter (TAC) through a delay. Now the output of the TAC was connected to the Analog to digital converter (ADC) and then to data acquisition system (DAQ). Here both the PMT connections up-to TAC were separate. At TAC for analyzing the signals the output (second output of TAC) was connected to the oscilloscope and the pulse was analyzed for different integrators and differentiator values (see table-3).

The circuit connection looks as follows:

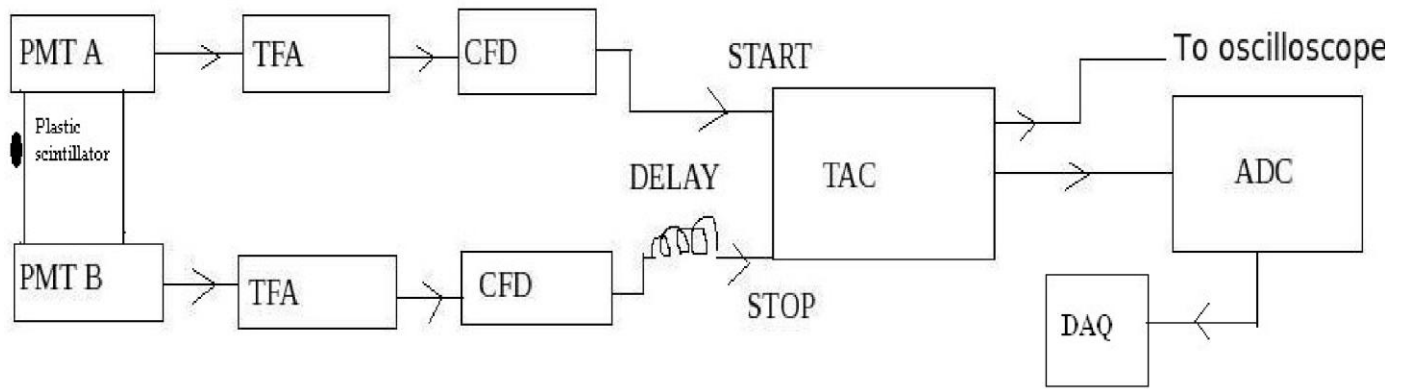


Fig-3: A block diagram of timing characteristics of the plastic scintillator.

Integrator (ns)	Differentiat or Out	Pulse height		Rise time		Decay time	
		Unprocess ed (mv)	Process ed (mv)	Unprocess ed (mv)	Process ed (mv)	Unprocess ed (mv)	process ed (mv)
20	20	15	300	2.5	10	12.5	50
20	20	15	180	2.5	7.5	12.5	25
20	50	15	260	2.5	10	12.5	25
20	100	15	300	2.5	10	12.5	40
50	50	15	160	2.5	10	12.5	45
50	100	15	160	2.5	10	12.5	50

Table 3: Variation of Pulse height, rise time decay time for different differentiator and integrator values.

Then we moved to constant fraction discriminator. A discriminator circuit selects the minimum pulse height above threshold and when the input pulse height exceeds the discriminator preset level, the discriminator generates an output.

Anode → TFA → Linear → Discriminator

These random fluctuations superimposed on the signal pulses of identical shape and size may cause the generation of output pulses at some what different time leading to a time jitter, often referred to as amplitude walk. Even if the input amplitude is constant such a walk can till take place, if change occur in the shape (i.e. rise time and the decay time) of the pulse. The CFD is used to overcome thee problems. For this a constant fraction of the total pulse irrespective of their amplitude reaches this point at the same time and hence pulses over a wide dynamic range can be accepted. This step involved in constant fraction timing is shown below.

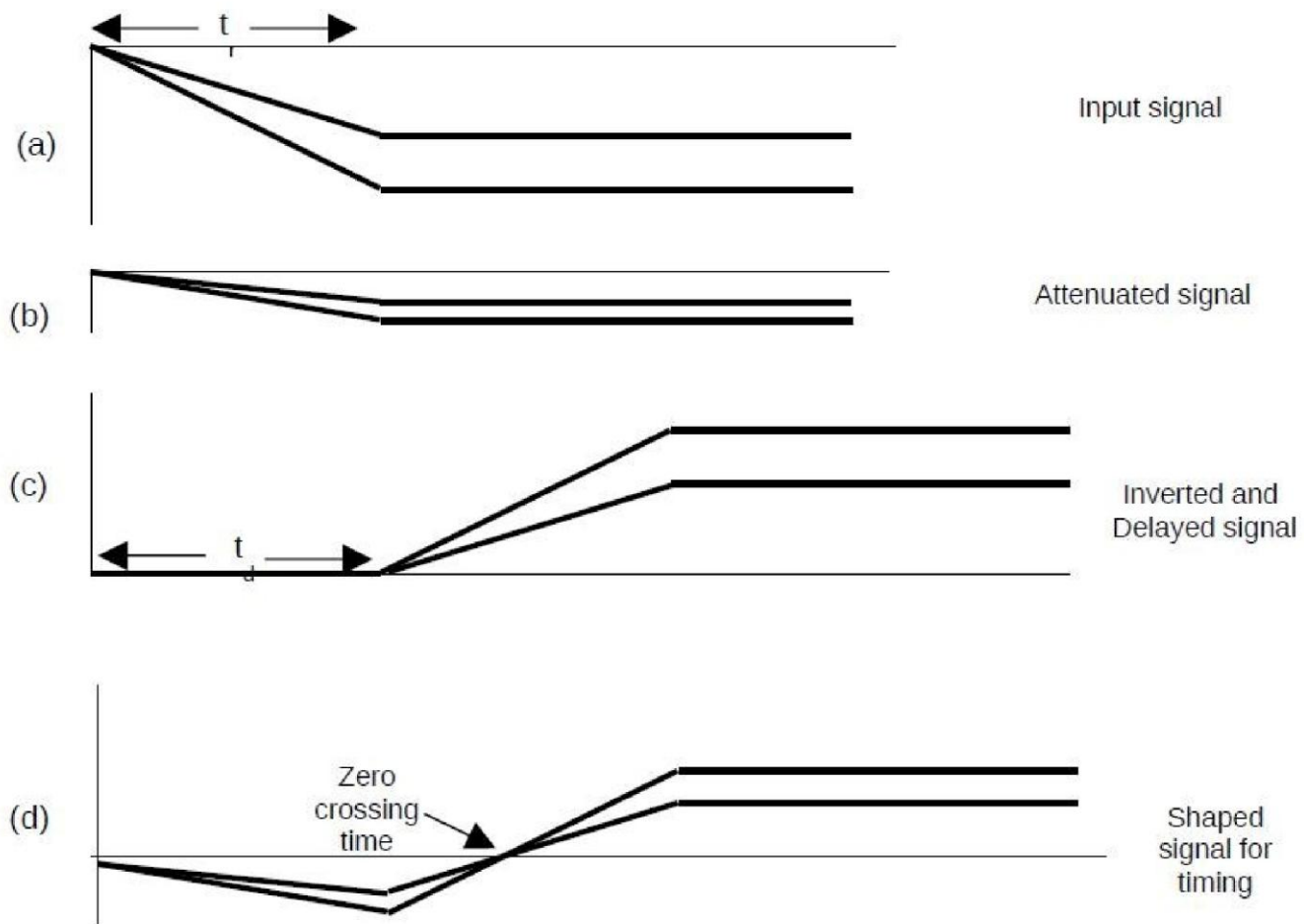


Fig 4: Waveforms in the constant fraction timing pick-off method. Only the leading edges of the pulses are shown above.

After getting familiarize with the functioning of the scintillator and some other electronic components like TFA, CFD and TAC, we moved to actual experiment with high purity germanium detector.

Experimental details:

A germanium semiconductor detector is a device that uses a germanium semiconductor to detect traversing charged particles or the absorption of photons. In the field of particle physics, these detectors are usually known as germanium detectors.

Germanium detectors are mostly used for spectroscopy in nuclear physics. Germanium can have a depleted, sensitive thickness of centimeters, and therefore can be used as a total absorption detector for gamma rays up to few MeV. These detectors are also called High-Purity Germanium detectors (HPGe) or Hyper pure Germanium detectors.

Germanium detectors are semiconductor diodes having a p-n structure in which the intrinsic region is sensitive to ionizing radiation, particularly x rays and gamma rays. Under reverse bias, an electric field extends across the intrinsic or depleted region. When photons interact with the material within the depleted region of the detector, charge carriers (holes and electrons) are produced and these are swept by the electric field to the p and n electrodes. This charge, which is in proportion to the energy deposited in the detector by the incoming photon, is converted into a voltage pulse by an integral charge sensitive preamplifier. These detectors have good energy resolutions but poor timing resolution.

The major drawback of Germanium detectors is that they must be cooled to liquid nitrogen temperatures to produce spectroscopic data. At higher temperatures, the electrons can easily cross the Band gap in the crystal and reach the conduction band, where they are free to respond to the electric field. The system therefore produces too much electrical noise to be useful as a spectrometer. Cooling to liquid nitrogen temperatures, 77.36 K reduces thermal excitations of valence electrons so that only a gamma ray interaction can give an electron the energy necessary to cross the band gap and reach the conduction band.

To start with the cooling of the detector, it is first flushed out with dry nitrogen gas for about 1 hour. After that liquid nitrogen is to be filled in the detector. Thereon the detector should be kept cooled to liquid nitrogen temperature till the experiment get over. This is done by filling liquid nitrogen in the detector at an interval of every 12 hours (Care should be taken to avoid the warm up of detector and also while filling). Once the experiment gets over the detector can be warmed up to room temperature.

In the germanium part of this project as a first step, we calibrated the energy corresponding to channels with the help of standard cobalt- 60 and Europium -152 source. For doing this we made the circuit as shown in the fig-5 (Note: The signal voltage to ADC should not exceed 10V). Here we adjusted the amplifier gain in such a manner that 10V input to ADC will correspond to 3MeV of particle energy. Then using the LAMPS software we collected the data for 15 minutes individually for both the cobalt and europium source and stored it separately.

We did calibration by identifying the channels corresponding to standard energy lines of the cobalt-60 (2 lines) and europium-152 (14 lines) in the stored files. We also took the data of FWHM and Area for resolution and relative efficiency calculations. The data's collected were given in table-4 below.

The calibration was done by considering all the 16 energy lines and plotting it in GNU plot with a fit of second order polynomial. The constants a , b , c was then entered into the calibration files of LAMPS software and stored as a separate file. Before doing this we created a text file containing Energy and peak channel for all the 16 lines as two separate columns, because GNU plot will accept only text files for plotting.

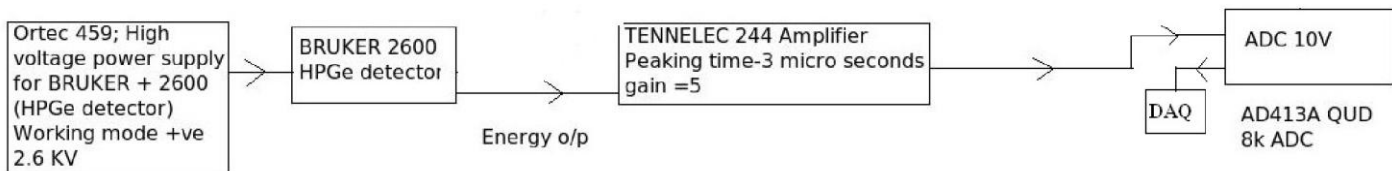


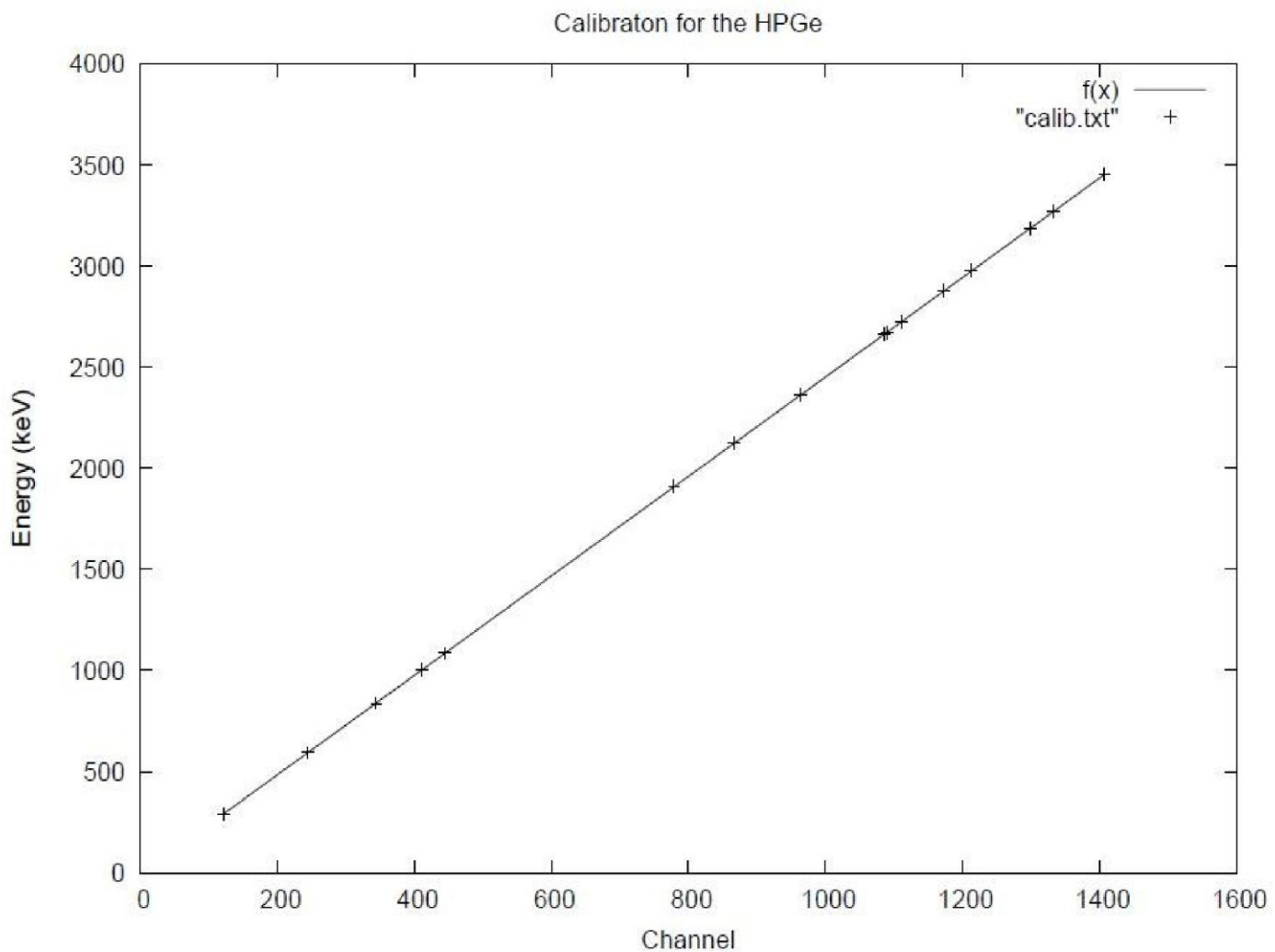
Fig-5: Block diagram for doing calibration

The Data's used for calculations were:

Energy (Kev)	Peak channel	FWHM	Area	Branching ratio	Error in energy	Error in FWHM	Error in area
<i>For europium -152</i>							
121.959	290	1.629	440080	0.2837	0.003	0.005	2815
244.649	593	1.699	80770	0.0753	0.004	0.009	656
344.07	838	1.779	219780	0.2657	0.002	0.004	632
410.83	1003	1.8	14880	0.02246	0.01	0.025	281
443.64	1084	1.867	19700	0.0312	0.006	0.013	193
778.867	1909	2.143	51250	0.1297	0.007	0.016	601
867.424	2127	2.205	14740	0.04214	0.1	0.023	235
964.141	2365	2.293	49400	0.1463	0.008	0.016	623
1085.96	2664	2.429	32600	0.1013	0.006	0.072	284
1089.87	2673	2.429	5220	0.01731	0.022	0.12	112
1112.19	2728	2.49	41740	0.1354	0.016	0.033	755
1213.04	2976	2.612	3890	0.01412	0.025	0.06	113
1299.27	3187	2.482	4240	0.01626	0.013	0.033	78
1408.07	3454	2.716	52600	0.2085	0.015	0.027	802
<i>For cobalt-60</i>							
1172.99	2877	2.473	40880		0.011	0.021	595
1332.17	3268	2.608	36800		0.013	0.023	619

Table 4 : Data's used for calibration of HPGe Detector.

The calibration graph looks as follows:



Graph 1: Plot of Energy Vs Channel number for Calibration.

The function used here is $f(x) = ax^2 + bx + c$

Here its found that the energy varies linearly with the channel number.

Then we calculated resolution and relative efficiency from the data's obtained.

The resolution is calculated by the formula

$$\text{RESOLUTION} = \text{FWHM}/\text{ENERGY}$$

Similarly the relative efficiency is calculated by the formula $R.E = (A1*B.R2)/(A2*B.R1)$

Where $B.R$ is the Branching ratio.

The calculated resolution and relative efficiency for each and every energy lines is below.

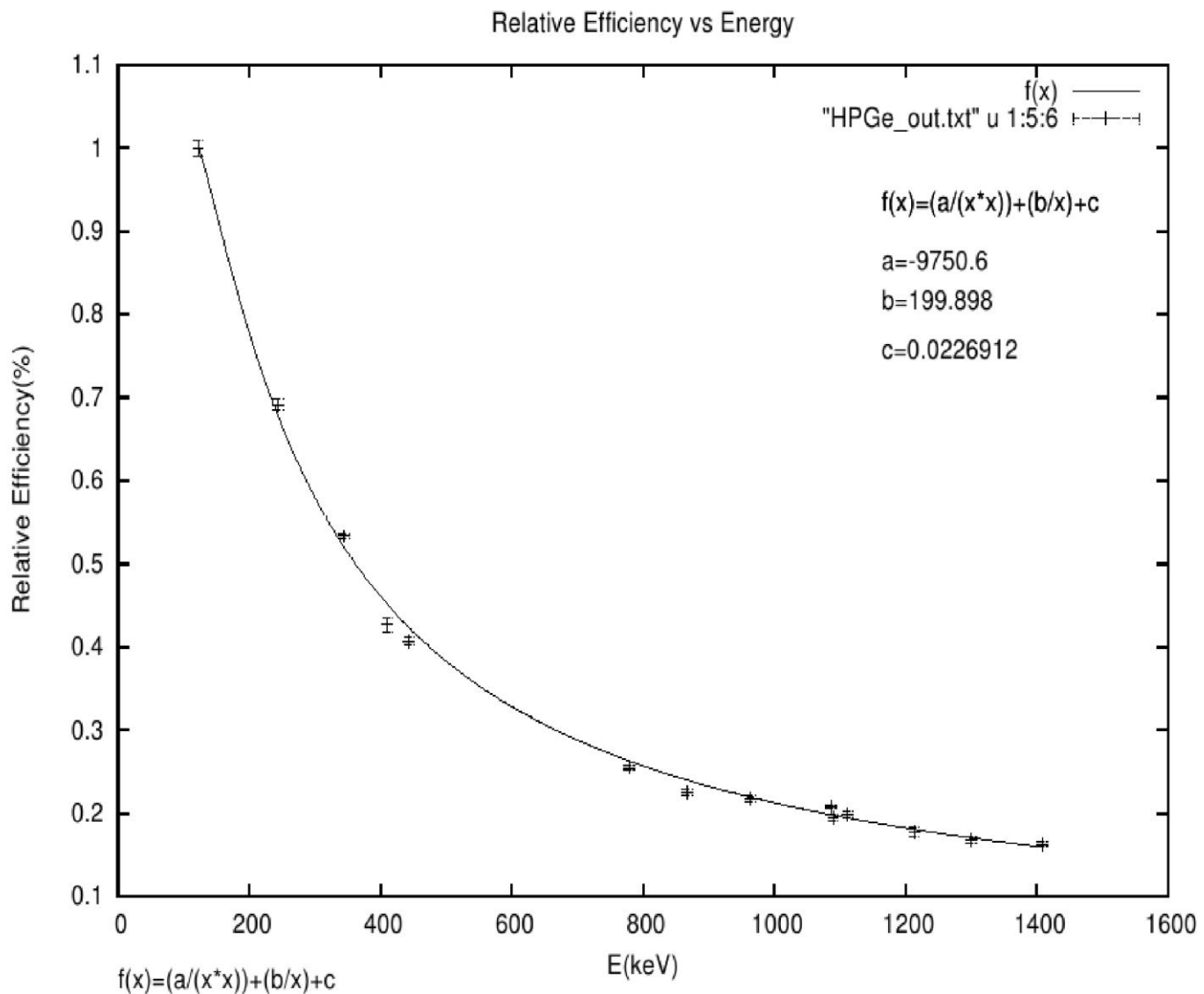
For Europium-152

Energy (Kev)	Resolution	Error in resolution	Relative efficiency	Error in relative efficiency
121.959	0.0133569	4.09987e-05	1	0.0090461
244.649	0.00694464	3.67876e-05	0.69149	0.0071488
344.07	0.00517046	1.16256e-05	0.53324	0.0037397
410.83	0.00438137	6.08525e-05	0.42709	0.0085155
443.64	0.00420837	2.93031e-05	0.40704	0.0047625
778.867	0.00275143	2.05427e-05	0.25473	0.0034027
867.424	0.00254201	2.65169e-05	0.22549	0.0038736
964.141	0.00237828	1.65951e-05	0.21768	0.0030781
1085.96	0.00223673	6.63008e-05	0.20746	0.0022422
1089.87	0.00222871	0.000110e-05	0.19440	0.0043525
1112.19	0.00223973	2.96712e-05	0.19873	0.0038128
1213.04	0.00215327	4.94625e-05	0.1776	0.0052827
1299.27	0.0019103	2053989e-05	0.16810	0.0032741
1408.07	0.00192888	1.91752e-05	0.16263	0.0026891

Table 5 : Shows resolution and relative efficiency with errors for different values of energy.

After calculating the resolution and relative efficiency for each and every line, we plotted it as a graph. It looks as follows.

Energy Vs Relative efficiency:

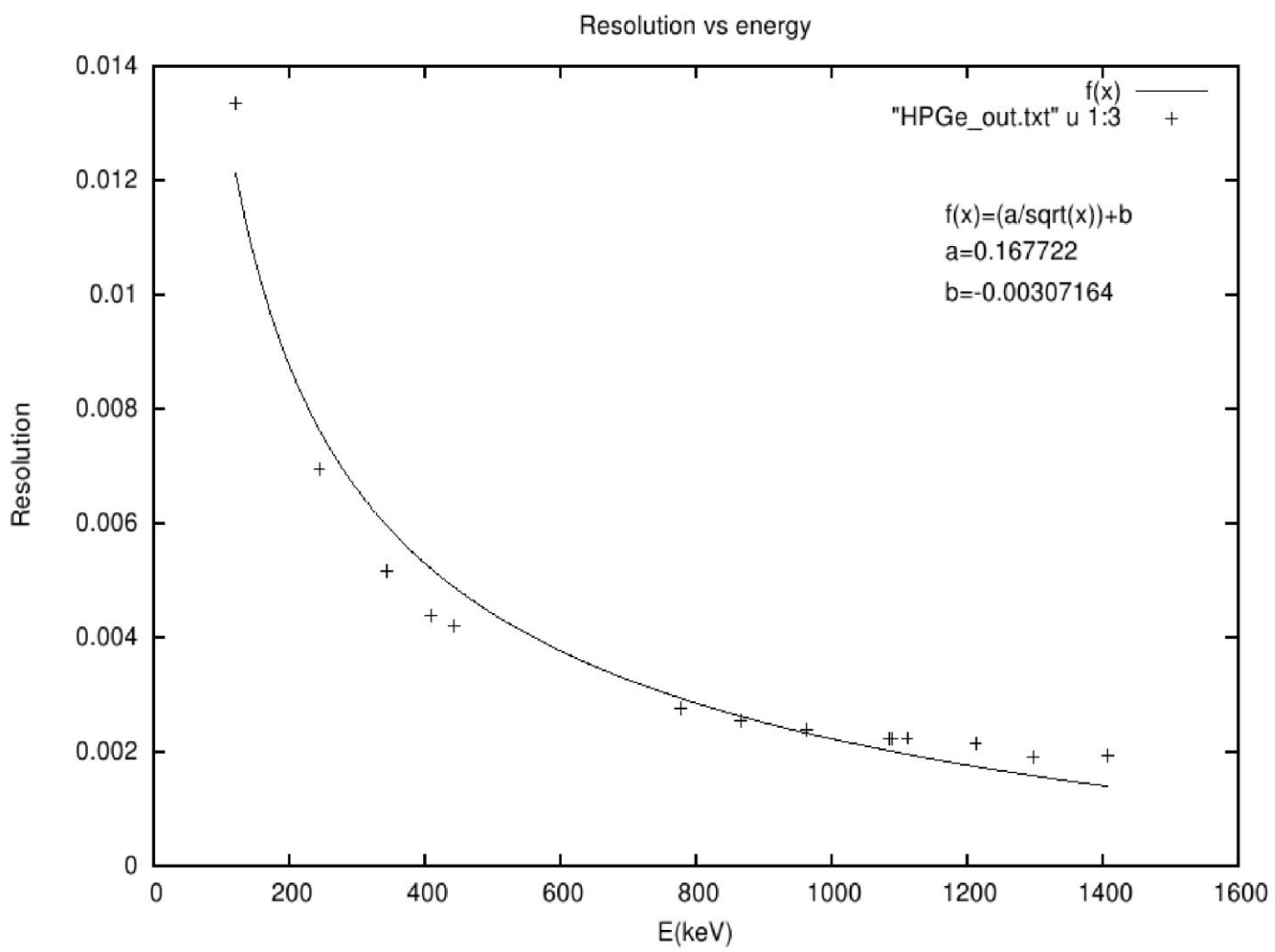


Graph 2: Plot of Relative efficiency Vs Energy.

The function used for this fit is $f(x) = (a/x^2) + (b/x) + c$

In general for any detector we know that the efficiency will decrease with an increase in energy. Here also we noted from the graph that the efficiency decreases with increase in energy.

Energy Vs Resolution:



Graph 3: Plot of Resolution Vs Energy.

The function used for this fit is $f(x) = (a/\sqrt{x}) + b$.

Here we noted that the resolution of the detector decreases with increase in energy. This implies that the detector can better resolve two or more energy lines having little difference in their energy.

Before doing the shielding for the germanium detector, we obtained the room background spectrum as 13 files (Amplifier gain: 10V corresponds to 3MeV of energy). Then we analyzed the room background spectrum by adding (using add 1D spectra option in LAMPS) 12 different files (out of the 13 files obtained for total duration of 30.12 hours) and identified the different energy lines, their source (see table-6) with the help of a standard spectrum.

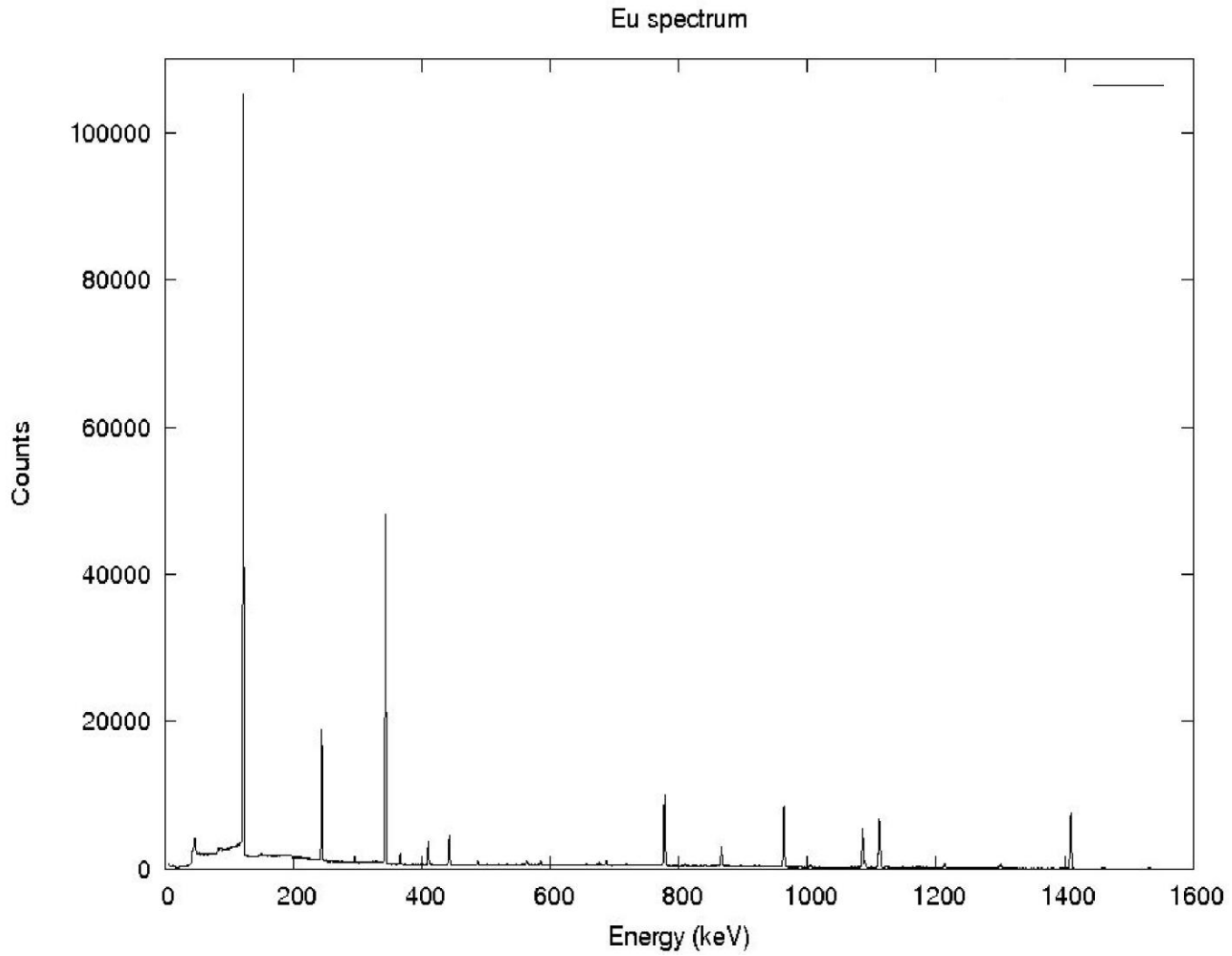


Fig-6: Europium 152 background spectrum

The different energy lines and their sources are tabulated below.

Source	E(KeV)	Source	E(KeV)
$^{235}U, ^{226}Ra$	186.2	^{228}Ac	964.9
^{228}Ac	209.5	^{228}Ac	1110.6
^{212}Pb	238.8	^{60}Co	1173.4
$^{224}Ra, ^{214}Pb$	241.7	^{214}Bi	1238.5
^{228}Ac	270.3	^{60}Co	1332.5
^{208}Tl	277.5	^{214}Bi	1378.0
^{214}Pb	295.3	^{214}Bi	1385.7
^{212}Pb	300.3	^{214}Bi	1402.1
^{228}Ac	328.0	^{214}Bi	1408.4
^{228}Ac	338.3	^{40}K	1461.2
^{214}Pb	352.0	^{228}Ac	1502.1
^{228}Ac	409.4	^{228}Ac	1588.5
^{228}Ac	462.7	^{208}Tl DE	1592.8
$^{208}Tl, ^{106}Ru$	510.5	^{212}Bi	1621.0
^{208}Tl	583.0	^{228}Ac	1631.1
^{214}Bi	609.2	^{214}Bi	1661.9
^{137}Cs	661.6	^{214}Bi	1730.0
^{214}Bi	665.3	^{214}Bi	1764.9
^{212}Bi	727.2	^{214}Bi	1847.7
^{208}Tl	763.3	^{208}Tl SE	2103.6
^{214}Bi	768.4	^{214}Bi	2118.9
$^{214}Bi, ^{214}Pb, ^{212}Bi$	785.8	^{214}Bi	2204.3
^{228}Ac	794.8	^{214}Bi	2447.6
^{208}Tl	860.6	^{208}Tl	2614.4
^{228}Ac	911.3		

Table 6: Shows Different energy lines and their sources.

Then the 12 files are added into a single file and stored in a different file name.

In the passive shielding part, we made a lead shielding to the germanium detector using lead bricks (5 cm thickness on all sides) and started data acquisition with the lead shield for 7 files of total duration 37.89 hours and these files were added into one file (different file name) using the add 1-d spectra option in the LAMPS software. The counts under different energy lines in the added file (with lead) were compared with the counts under the added background file (without lead) and the reduction factor for each energy was found (see table-7).

Gamma energy (keV)	With Lead Counts/hr(A)	Without Lead Counts/hr(B)	B/A
75.3	348±34	625±195	1.79±0.58
93.4	89±12	858±131	10±2
186.2	103±10	1489±136	14±2
209.5	84±15	721±145	9±2
238.8	104±11	6815±230	66±7
510.5	211±10	3316±84	15.72±0.85
583.0	34±6	3935±69	116±21
661.6	226±9	4817±91	21.31±0.94
1332.5	11±4	447±30	41±15
1461.2	183±8	15069±236	82±4
1764.9	22±3	1287±42	59±8
1847.7	1.5±0.9	152±15	101±61
2103.6	2±1	426±25	213±107
2204.3	6±2	366±18	61±21
2614.4	89±2	3181±88	35.74±1.27

Table 7: Shows Reduction for Different energy lines with lead shield.

The background Spectrum with and without lead are shown in fig-7:

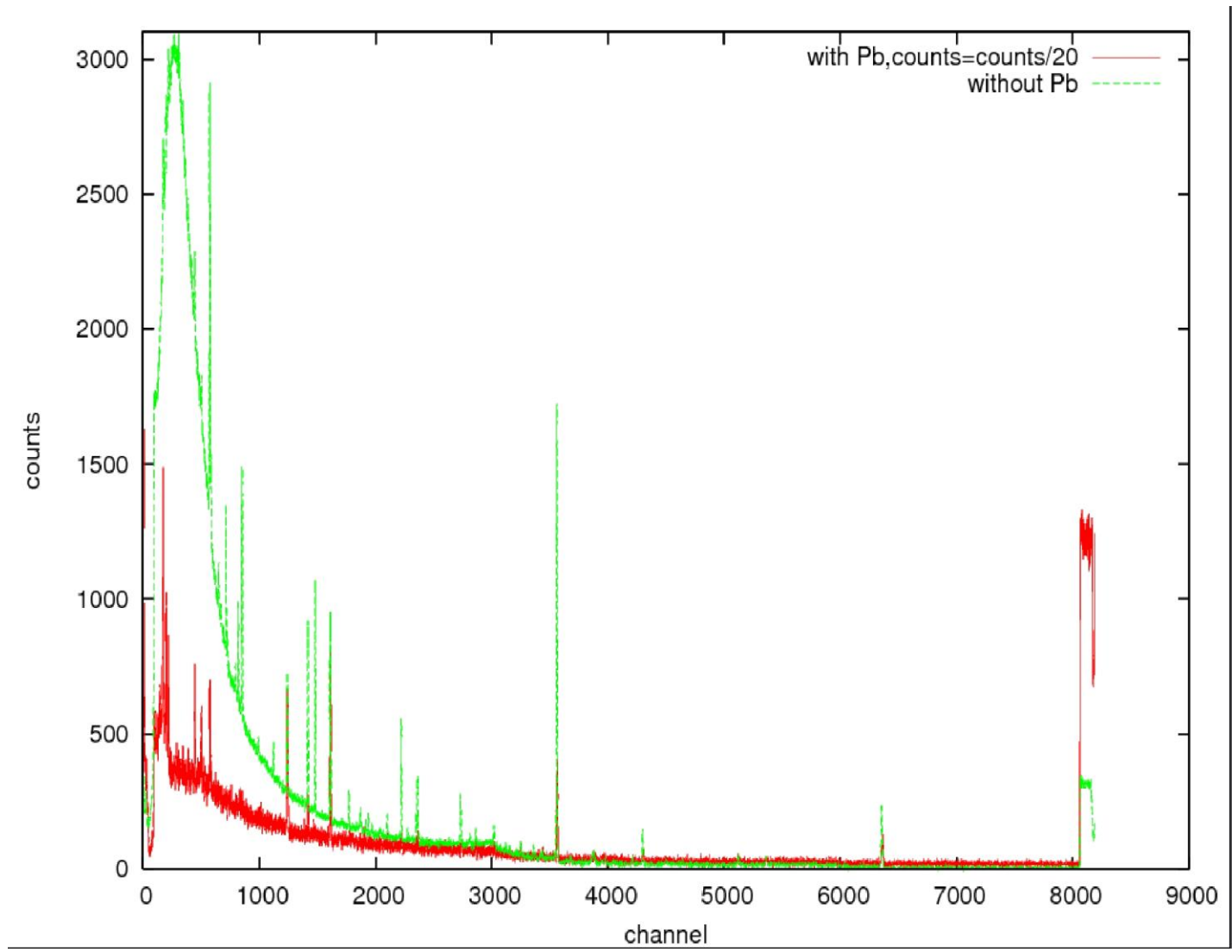


Fig-7: Super imposed with and without background spectrum

In the active shielding part of this project, we set up a veto shield to the HPGe detector with the help of plastic scintillator and a PMT. In this set up the scintillator is kept on the top of the germanium detector (without touching the detector) with the help of supports. The basic thing here is that we provided an Anti-coincidence logic (i.e. If we get signals on both the scintillator and detector then we want to neglect that counts because these particles are high energy cosmic ray muon's and if we get signal only in HPGe detector then we have taken that count into account). This Anti-coincidence logic is set up with the help of basic gates like AND, OR, NOT. In order to achieve this we made the circuit as shown in fig-8.

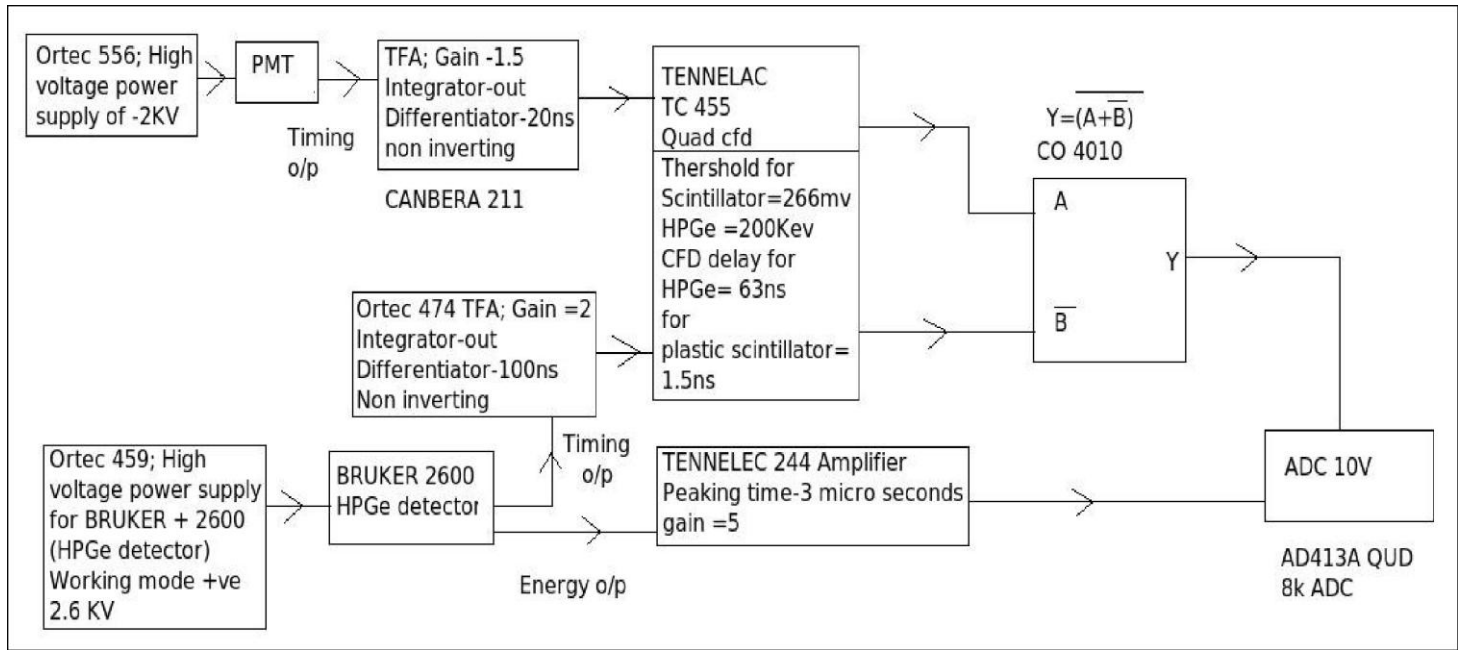


Fig-8: Block diagram for anti-coincidence set-up.

After doing all the preliminary adjustments like pole zero settings and width settings, we started the background data acquisition (with veto enabled) in batch file mode for 9 files of total duration 29.79 hours. Similarly after completing this we did data acquisition for background with veto disabled in batch file mode for 4 files of total duration 6.33 hours. Initially in active shielding part the amplifier gain was adjusted, such that 10V to ADC will correspond to 12Mev of energy. We did this in order to detect the high energy rays in the background.

In the next step these files (with veto enabled) were added (Care should be taken for shifts of energy line in different files) to one single file with the help of add 1-d spectra option present in LAMPS software and saved in a different file. Similarly veto disabled files were also added and stored in a different file name. Then the counts for the energy range of 3-5 Mev, 5-10 Mev, and for the energy lines of 1461, 2615 were normalized to per hour counts and compared for veto enabled and veto disabled spectrum (see table-8).

Energy range	Counts per hour with veto disabled	Counts per hour with veto enabled	Reduction
3-5 MeV	202	129	0.64
5-10 MeV	306	165	0.54
1461 KeV	303	256	0.85
2615 KeV	70	62	0.90

Table 8: Shows the reduction for different energy range with active cosmic veto.

Then we calculated the energy deposited by the cosmic ray muon in the plastic scintillator and HPGe detector separately. For doing this we measured the dimensions of the plastic scintillator (41cm x 41cm x 9cm) and HPGe detector crystals (Diameter =5cm and length=7.5 cm).

The average energy of muon at sea level is 4GeV and flux at sea level is given by one muon/cm²/min. The energy loss of a 4GeV muon traveling through matter is 1.8MeV/g/cm².

The dimension of plastic scintillator used is (41cmX41cmX9cm) and the density (ρ) of plastic scintillator material (PVT) is 1.05g/cm³. Assuming that most of the muons are directed downward,

$$\rho \cdot t = 9.45 \text{ gm/cm}^2$$

$$\begin{aligned} \text{So energy deposited by one muon} &= 1.8 \text{ MeV/gm/cm}^2 \times 9.45 \text{ gm/cm}^2 \\ &= 17.01 \text{ MeV} \end{aligned}$$

The diameter of HPGe Crystal is 5cm. and the length is 7 cm and the density of Ge is 5.323gm/cm³.

$$\begin{aligned} \rho \cdot t &= 5.323 \text{ gm/cm}^3 \times 5 \text{ cm} \\ &= 26.615 \text{ gm/cm}^2 \end{aligned}$$

So maximum energy deposited by one muon,

$$\begin{aligned} &= 1.8 \text{ MeV/gm/cm}^2 \times 26.615 \text{ gm/cm}^2 \\ &= 53.23 \text{ MeV} \end{aligned}$$

The maximum energy detected in the experiment= 10MeV

The thickness of HPGe at which 10MeV is deposited, $t' = 10 \text{ MeV} \times 5 \text{ cm} / 53.23 \text{ MeV}$
 $= 0.939 \text{ cm}$

Conclusion:

From the analyses done with the data's collected, we observed that by doing the passive and active shielding for the HPGe detector the low background and high background radiations respectively are minimized and this shows that it is possible for us to measure the intrinsic background radiations of the detector to a high level of accuracy.

Teams:

- 1) A.Thirunavukarasu,
- 2) Lakshmi.s.mohan,
- 3) Meghna.K.K,
- 4) Maulik nariya.

References:

- 1) "Radiation detection and measurements" by Glenn F. Knoll, Wiley India Edition 2000.
- 2) "Techniques for nuclear and particle physics experiments: a-how-to approach" by William R. Leo. Narosa publishing house, New Delhi.
- 3) F.Pointurier, J.Laurec, X.Blauchard and A.Adam, APPL, Radiat Isot vol.47 No-9/10, pp-1043-1048, 1996